
Privacy-Preserving Data Release Leveraging Optimal Transport and Particle Gradient Descent

Konstantin Donhauser^{*1} Javier Abad^{*1} Neha Hulkund² Fanny Yang¹

Abstract

We present a novel approach for differentially private data synthesis of protected tabular datasets, a relevant task in highly sensitive domains such as healthcare and government. Current state-of-the-art methods predominantly use marginal-based approaches, where a dataset is generated from private estimates of the marginals. In this paper, we introduce PrivPGD, a new generation method for marginal-based private data synthesis, leveraging tools from optimal transport and particle gradient descent. Our algorithm outperforms existing methods on a large range of datasets while being highly scalable and offering the flexibility to incorporate additional domain-specific constraints.

1. Introduction

Distributing sensitive datasets is crucial for data-driven decision-making and methodological research in many fields, including healthcare and government. For example, epidemiologists and biostatisticians have relied on tools like SAS to analyze personal health data for decades (Dankar & El Emam, 2012; DiMaggio, 2013). However, there are significant concerns among patients about the use and disclosure of their information, especially among vulnerable groups (El Emam, 2011).

Differential privacy (DP) has gained prominence as a vital approach to mitigate privacy concerns. Its adoption extends well beyond theoretical frameworks, finding practical utility across industries and government organizations (Johnson et al., 2018; Abowd, 2018; Aktay et al., 2020). In this paper, we target the problem of differentially private tabular data synthesis, a promising approach for creating high-quality copies of protected tabular datasets that adhere to privacy

constraints. Any further task performed on these “private” copies is thus guaranteed to comply with these constraints.

Numerous differential privacy methods have emerged to synthesize tabular datasets with privacy guarantees while preserving relevant statistics from the original dataset (Tao et al., 2021; Hu et al., 2024). Marginal-based approaches are among the preferred methods, dominant in NIST challenges (McKenna et al., 2021) and consistently top-ranked in benchmarks (Tao et al., 2021). These approaches select a set of marginals and perturb them in a DP-compliant manner. Subsequently, a synthetic dataset is *generated* from these noisy marginals through a generation method.

In this paper, we introduce PrivPGD¹, a novel DP-data generation method based on particle gradient descent (Chizat & Bach, 2018; Chizat, 2022). PrivPGD leverages an optimal transport-based divergence between the privatized and particle marginal distributions (Section 2.2) to integrate marginal information during gradient descent. This divergence can be efficiently approximated through parallel GPU processing, which is crucial for handling large datasets. Our approach has several important characteristics:

- *State-of-the-art performance.* PrivPGD outperforms state-of-the-art methods in a large benchmark comparison (9 datasets) across a wide range of metrics, including downstream task performance (Section 4).
- *Scalability.* PrivPGD leverages a highly optimized gradient computation that can be parallelized on GPU, enabling the algorithm to efficiently construct large datasets with over 100,000 data points while accommodating many marginals, e.g., all 2-Way marginals.
- *Geometry preservation.* Many datasets contain features with inherent geometry, such as continuous features and some categorical features like age, which have rankings that should be retained in the synthetic data. Unlike state-of-the-art methods (see Section 4.2), PrivPGD preserves this geometric structure, aligning more naturally with the nuances of real-world datasets.

^{*}Equal contribution ¹Department of Computer Science, ETH, Zurich, Switzerland ²MIT CSAIL, Boston, USA. Correspondence to: Konstantin Donhauser <konstantin.donhauser@ai.ethz.ch>, Javier Abad <javier.abadmartinez@ai.ethz.ch>.

¹See our GitHub repository for the source code: <https://github.com/jaabmar/private-pgd>.

- *Incorporation of domain-specific constraints.* As a gradient-based method, PrivPGD allows the inclusion of any additive penalization term to the loss function. This enables explicit enforcement of domain-specific constraints within the generation algorithm, providing a straightforward and efficient method to incorporate these requirements into the synthetic data. Examples and successful implementations of such constraints are provided in Section 4.4.

1.1. Related work

In this section, we discuss related works on DP-data synthesis for tabular data and direct the readers to Section 4 for extensive benchmark comparison. For a comprehensive overview, refer to the recent survey by Hu et al. (2024). We categorize the related work into marginal and query-based DP-data synthesis algorithms. Query-based algorithms handle a broad set of queries, while marginal-based algorithms focus on marginal queries and can be seen as a special case of query-based algorithms optimized for these queries.

Marginal-based algorithms Marginal-based algorithms are prominent in the literature for private tabular data synthesis, achieving state-of-the-art performance on numerous benchmark tasks (McKenna et al., 2021; Tao et al., 2021; Hu et al., 2024). These algorithms typically follow two main steps: selecting marginals (Cai et al., 2021; McKenna et al., 2021; 2022) and generating the dataset after adding noise to these marginals (Zhang et al., 2017; McKenna et al., 2019; Li et al., 2021). A common approach in data generation is PGM, used by winning methods in the NIST competitions (Cai et al., 2021; McKenna et al., 2021; 2022). Nonetheless, PGM has limitations, including sensitivity to the number of selected marginals, which can lead to memory and runtime issues, and a limited ability to preserve domain-specific constraints. Other generation methods include PrivBayes (Zhang et al., 2017), which trains a Bayesian network, and Gradual Update Methods (GUM) (Li et al., 2021; Zhang et al., 2021), which iteratively update a random dataset to match the marginals.

Query-based algorithms In contrast to marginal-based algorithms, query-based algorithms can handle a broader range of queries. Examples include DualQuery (Gabori et al., 2014), FEM (Vietri et al., 2020), RAP (Aydore et al., 2021), GEM (Liu et al., 2021), RAP++ (Vietri et al., 2022), and Private GSD (Liu et al., 2023). These methods construct a private dataset to efficiently answer a large set of predefined queries, often relying on gradient descent techniques (Aydore et al., 2021; Liu et al., 2021). Our method, PrivPGD, also uses particle gradient descent but does not require predefining a set of queries and is optimized to preserve marginal queries.

Other algorithms Generative Adversarial Networks (GANs) have been proposed for synthesizing private data (Xie et al., 2018; Jordon et al., 2019; Torkzadehmahani et al., 2019). However, similar to other generator-based approaches (Liu et al., 2021; Vero et al., 2023), they require specifying and tuning a parametric model, a challenging task due to the high sensitivity to hyperparameters. Conversely, our method, PrivPGD, leverages particles to represent data, avoiding the need for model selection and tuning, and is remarkably robust to hyperparameter selection. Additionally, GANs reportedly fail to preserve basic distributional statistics for tabular datasets (Tao et al., 2021). Furthermore, DP-Sinkhorn (Cao et al., 2021), an optimal transport-based generative method, cannot be easily extended to tabular data synthesis. DP-SWD (Rakotomamonjy & Liva, 2021), a differentially private measure based on the sliced Wasserstein distance, has been used for training generative models (Rakotomamonjy & Liva, 2021; Sebag et al., 2023). Lastly, copula-based approaches (Li et al., 2014; Asghar et al., 2019; Gambs et al., 2021) employ Gaussian and vine copulas to model the privatized marginal distributions, but these methods are computationally intensive. For example, executing a single iteration of Copula-Shirley (Gambs et al., 2021) on the ACS datasets (Ding et al., 2021) takes over 24 hours on our cluster².

2. Preliminaries for Differentially Private Data Synthesis

In this section, we summarize key concepts and introduce notation related to differentially private data synthesis.

In general, we consider our data to lie in a domain $\mathcal{X} = \mathcal{X}_1 \times \dots \times \mathcal{X}_d$ that is discrete and has dimension d . This assumption is not restrictive since the vast majority of DP-data synthesis algorithms for tabular data rely on a discretized version of the data even if it originally lies in a continuous domain³. In particular, we can represent every dimension as an integer in the discrete set $\mathcal{X}_i = \{1, \dots, k_i\}$ with $k_i \in \mathbb{N}_+$.

Differential privacy (Dwork, 2006) is an algorithmic property that guarantees that individual information in the data is protected in the output of an algorithm; even when assuming that an adversary has access to the information of all other individuals in the dataset. We now provide the formal definition.

²Our cluster consists of modern GPUs, at least of the NVIDIA GeForce RTX 2080 Ti type, and we used the official implementation from <https://github.com/alxxrg/copula-shirley>.

³We refer the reader to (Zhang et al., 2016) for a discussion on how to optimally discretize in a DP-way.

Algorithm 1 Standard data synthesis framework

Require: Dataset D , privacy parameters ϵ and δ

- 1: **select** set \mathcal{S} of subsets S of $\{1, \dots, d\}$
- 2: **privatize** marginals $\nu_S[D]$ to obtain (ϵ, δ) -DP “copies” $\hat{\nu}_S$
- 3: **generate** data from privatized marginals $\hat{\nu}_S$

return the DP dataset D_{DP}

Definition 2.1. An algorithm \mathcal{A} is (ϵ, δ) -DP with $\epsilon > 0$ and $\delta > 0$ if for any datasets D, D' differing in a single entry and any measurable subset $S \subset \text{im}(\mathcal{A})$ of the image of \mathcal{A} , we have

$$\mathbb{P}(\mathcal{A}(D) \in S) \leq \exp(\epsilon)\mathbb{P}(\mathcal{A}(D') \in S) + \delta$$

The goal of *differentially private data synthesis* is to design a (randomized) algorithm \mathcal{A} that, for any dataset $D \in \mathcal{X}^n$ of size n , generates an output $\mathcal{A}(D) \in \mathcal{X}^m$ that is a differentially private “copy” of D , potentially with size $m \neq n$.

2.1. Marginal-based algorithms for private data synthesis

Our approach falls in the general category of marginal-based methods. They follow Algorithm 1, consisting of three steps: marginal selection, privatization, and generation.

Marginal selection For any subset $S \subset \{1, \dots, d\}$ of the dimensions, we denote with $D_S \in \mathcal{X}_S^n$ the dataset containing only the dimensions in S . For each subset S we can define a corresponding marginal.

Definition 2.2. We denote by $\nu_S[D] \in \mathcal{P}(\mathcal{X}_S)$ the S -marginal of a dataset D , defined as the empirical measure of D_S over the domain \mathcal{X}_S .

In the first step of the algorithm, a set \mathcal{S} of such subsets S is selected, and equivalently a set of marginals. The problem of selecting marginals in a DP-way is an interesting problem on its own and has led to a significant amount of proposed methods (Cai et al., 2021; Zhang et al., 2021; McKenna et al., 2021; 2022). In an extension of Algorithm 1, sketched in Algorithm 2, the marginals are not all selected in the beginning, but sequentially chosen from a pre-defined pool of subsets \mathcal{S}_W of $[d]$ (often referred to as the workload). More specifically, in every iteration t , we select the marginals with the largest total variation distance $\text{TV}(\nu_S[D_{\text{DP}}^{(t-1)}], \nu_S[D])$, where $D_{\text{DP}}^{(t-1)}$ is the DP-dataset from the previous iteration $t - 1$. This is done in a DP-way using the exponential mechanism (McSherry & Talwar, 2007). Such approaches fall under the general MWEM (Hardt et al., 2012; Liu et al., 2021) framework, which is the backbone of many DP synthesis methods. To control the overall privacy budget, the framework from Algorithm 2 uses advanced compositional theorems (see e.g., (Dwork & Roth, 2014)).

Algorithm 2 Extension to sequential query selection

Require: Dataset D , privacy parameters ϵ and δ , workload \mathcal{S}_W , rounds T

- 1: **for** $t = 1, \dots, T$ **do**
- 2: **select** $S_t \in \mathcal{S}_W$
- 3: **privatize** the marginal $\nu_{S_t}[D]$ to obtain the DP-“copies” $\hat{\nu}_{S_t}$
- 4: **generate** data from privatized marginals $\{\hat{\nu}_{S_j}\}_{j \leq t}$ to obtain $D_{\text{DP}}^{(t)}$
- 5: **end for**
- 6: **return** DP dataset $D_{\text{DP}}^{(T)}$

Marginal privatization After a set of marginals has been selected, both frameworks contain a privatization and generation step. A common choice for privatization is to apply the Gaussian mechanism (McSherry & Talwar, 2007), where we simply add i.i.d. Gaussian noise to the empirical marginal $\nu_S[D]$. The variance σ^2 of the Gaussian depends on the privacy parameters ϵ and δ . As a result, we obtain the signed measures $\hat{\nu}_S$:

$$\forall x \in \mathcal{X}_S : \hat{\nu}_S(\{x\}) = \nu_S[D](\{x\}) + \mathcal{N}(0, \sigma^2).$$

Data generation Finally, in the last step, we generate a dataset from the noisy estimates of the marginals. For this purpose, existing methods typically aim to learn a distribution \hat{p} that minimizes the squared loss:

$$\sum_{S \in \mathcal{S}, x \in \mathcal{X}_S} (\hat{p}_S(\{x\}) - \hat{\nu}_S(\{x\}))^2$$

and then release the private synthetic data D_{DP} by sampling from \hat{p} . The predominant generation algorithm used by state-of-the-art methods (Cai et al., 2021; McKenna et al., 2021; 2022) is PGM (McKenna et al., 2019), which learns a graphical model using mirror descent (see Section 1.1).

2.2. Sliced Wasserstein distance

The optimal transport literature offers a set of natural divergence measures that can be used for particle gradient descent, such as the Sinkhorn divergence or the Wasserstein distance. However, the computational complexity of these divergences scales at least quadratically (resp. cubically) with respect to the size of the support of the measures. This clearly defeats the purpose of a computationally efficient generation algorithm that can represent rich datasets with a large number of data points. Instead, a widely used (Kolouri et al., 2018; Deshpande et al., 2018; Wu et al., 2019; Deshpande et al., 2019), computationally efficient alternative is the squared sliced Wasserstein (SW_2^2) distance (Bonneel et al., 2015); that is, the averaged squared Euclidean transportation over all 1-dimensional projections.

Formally, for $\theta \in \mathbb{R}$, let $g^\theta(x) = \langle x, \theta \rangle$ and $g_{\#}^\theta$ be the pull-back measure induced by g^θ . Moreover, let λ^p be the uniform distribution over the sphere \mathcal{S}^{p-1} . For any Euclidean subspace $\Omega \subset \mathbb{R}^p$ and probability measures $\mu, \nu \in \mathcal{P}(\Omega)$ with support Ω , the q -SW distance is defined as follows:

$$\text{SW}_q(\mu, \nu) = \left(\int_{\mathcal{S}^{p-1}} W_q^q(g_{\#}^\theta \mu, g_{\#}^\theta \nu) d\lambda(\theta) \right)^{1/q}, \quad (1)$$

where W_q^q is the q -th power of the q -Wasserstein distance for $q \geq 1$. The Wasserstein distance over 1-dimensional distributions, as it appears in Equation (1), has a well-known closed-form expression:

$$W_q(g_{\#}^\theta \mu, g_{\#}^\theta \nu) = \left(\int_u |F_{g_{\#}^\theta \mu}^{-1}(u) - F_{g_{\#}^\theta \nu}^{-1}(u)|^q du \right)^{1/q}, \quad (2)$$

where $F_{g_{\#}^\theta \mu}(u)$ (resp. $F_{g_{\#}^\theta \nu}(u)$) represents the cumulative function and F^{-1} its inverse. Finally, in the special case of $q = 1$, we have the following identity for the 1-Wasserstein distance by Vallender (1974), which we will later leverage in our algorithm:

$$W_1(g_{\#}^\theta \mu, g_{\#}^\theta \nu) = \|F_{g_{\#}^\theta \mu}(u) - F_{g_{\#}^\theta \nu}(u)\|_{L_1(\mathbb{R})}. \quad (3)$$

Importantly, this identity allows us to naturally extend the definition of the (sliced) 1-Wasserstein distance to signed measures, as demonstrated by Boedihardjo et al. (2022).

3. PrivPGD: a Particle Gradient Descent-Based Generation Method

We introduce *PrivPGD* (Algorithm 3), a novel approach for solving the generation step in marginal-based tabular data synthesis (Algorithm 1). Unlike other marginal-based methods (Zhang et al., 2017; McKenna et al., 2019), PrivPGD does not construct a dataset by sampling from a learned distribution. Instead, it directly propagates particles in an embedding space to minimize the sliced Wasserstein distance. A distinct advantage is that, through particle gradient descent, we can easily enforce domain-specific constraints by adding a penalization term $\hat{\mathcal{R}}$ to the loss. A similar approach for incorporating domain-specific constraints has recently been proposed for generator-based data synthesis algorithms (Vero et al., 2023), where the authors provide various examples of such losses.

In summary, our data generation method returns a DP-dataset D_{DP} given the following inputs:

1. A set of differentially private finite signed measures $\{\hat{\nu}_S\}_{S \in \mathcal{S}}$ constructed as in Algorithm 1.
2. A differentially private regularization loss $\hat{\mathcal{R}}$ incorporating domain-specific constraints.

Algorithm 3 Private Particle Gradient Descent

Require: DP marginals $\{\hat{\nu}_S\}_{S \in \mathcal{S}}$, regularizer $\hat{\mathcal{R}}$, number of particles m

- 1: **projection:** $\forall S \in \mathcal{S}$, construct the empirical measures $\hat{\mu}_S$ from $\hat{\nu}_S$
- 2: **optimization:** randomly initialize $Z^{(0)} \in \Omega^m$
- 3: **for** $t = 1, \dots, T$ **do**
- 4: **select** batch $\mathcal{S}_{\text{batch}} \subset \mathcal{S}$
- 5: **compute** the gradient at $Z^{(t-1)}$ of

$$\sum_{S \in \mathcal{S}_{\text{batch}}} \text{SW}_2^2(\mu_S[Z], \hat{\mu}_S) + \lambda \hat{\mathcal{R}}(Z)$$

- 6: **update** $Z^{(t)}$ using any first order optimizer
 - 7: **end for**
 - 8: **finalization step:** construct D_{DP} from $Z^{(T)}$
 - return** DP dataset D_{DP}
-

3.1. Preliminaries: Embedding

PrivPGD crucially relies on an embedding $\text{Emb} : \mathcal{X} \rightarrow \Omega$ of the (discretized) domain \mathcal{X} into a compact Euclidean product space $\Omega = \Omega_1 \times \dots \times \Omega_d$. We simply choose $\Omega = [0, 1]^d$ and map every $x \in \mathcal{X}$ to equally-spaced centers

$$\text{Emb}(x)_i = \frac{2x_i - 1}{2k_i} \in [0, 1]. \quad (4)$$

This choice of embedding preserves the order in \mathcal{X} , which is essential for variables such as age or any discretized continuous variables. In line with common practices in the literature (McKenna et al., 2021; Tao et al., 2021), we discretize continuous data using equally spaced bins. This method ensures that the embedding accurately represents the scaled distances between the centers.

We acknowledge that features like race, where imposing an ordering might be inappropriate, could be embedded into the space $[0, 1]^2$ so that the centers are equidistant. Similarly, when embedding categorical variables representing locations, an embedding that preserves geographical distances might be preferable. While it would be interesting to explore other embeddings, we leave it to future work.

Particles PrivPGD aims to construct m data points in the embedding space, ensuring their empirical distribution closely approximates the projection of the privatized signed measure $\hat{\nu}_S$. For any set of points $Z \in \Omega^m$, which we also refer to as the m particles, we define $Z_S \in \Omega_S^m$ as the projection of these particles onto the embedding Ω_S of \mathcal{X}_S . Moreover, we define S -marginals over Ω as:

Definition 3.1. We denote by $\mu_S[Z] \in \mathcal{P}(\Omega_S)$ the S -marginal of the particles Z , defined as the empirical measure of Z_S over the domain Ω_S .

3.2. Projection step

The preliminary embedding step allows us to define the particles Z within a convenient domain Ω , which we choose to be the hypercube with a fixed grid. In the projection step, the goal is to transform the privatized signed measure $\hat{\nu}_S$ into a proper probability measure $\hat{\mu}_S$ that can be “plugged into” the Wasserstein distance. Further, since we aim to find particles whose empirical distribution closely approximates the signed measure, we quantize $\hat{\mu}_S$ using the same number of particles, m .

Projection First, note that the embedding Emb from Equation (4) defines corresponding finite signed measures $\hat{\omega}_S$ over $\text{Emb}(\mathcal{X})_S \subset \Omega_S$ for each privatized signed measure $\hat{\nu}_S$. However, the sliced Wasserstein distance that we minimize in the optimization step (Section 3.3) is defined for probability measures. For $q = 1$ we can extend the sliced 1-Wasserstein distance from Equation (3) to signed measures and obtain a probability measure. Inspired by [Boedihardjo et al. \(2022\)](#) (see also ([Donhauser et al., 2023](#))), we transform by solving

$$\hat{\omega}_{S,\mathbb{P}} = \arg \min_{w \in \mathcal{P}(\text{Emb}(\mathcal{X})_S)} \text{SW}_1(w, \hat{\omega}_S). \quad (5)$$

We approximate this convex optimization problem using gradient descent. We also approximate the integral in SW_1 using Monte Carlo samples. Importantly, minimizing the objective in Equation (5) allows for preserving the geometry from the signed measures in the probability measures.

Quantization We further quantize the finite probability measures $\hat{\omega}_{S,\mathbb{P}}$ using m particles $\hat{Z}_S \in \Omega_S^m$, i.e.,

$$\hat{\mu}_S = \frac{1}{m} \sum_{i=1}^m \delta[\hat{Z}_S^i], \quad (6)$$

such that $\hat{\mu}_S \approx \hat{\omega}_{S,\mathbb{P}}$. This can be achieved by using any standard quantization technique with a negligible error for a sufficiently large number of particles. We apply the quantization in Equation (6) with m particles, thus ensuring that both $\mu_S[Z]$ and $\hat{\mu}_S$ are empirical measures over the same number of particles.

3.3. Optimization and finalization step

In the optimization step, we aim to generate a dataset by finding particles $Z \in \Omega^m$ that are close to the differentially private measure $\hat{\mu}_S$ constructed in the projection step. In particular, the final particles should minimize the squared sliced Wasserstein distance SW_2^2 (Equation (1)) between the empirical marginal distributions of the particles $\mu_S[Z]$ and $\hat{\mu}_S$. We additionally incorporate domain-specific constraints via a DP differentiable penalty term $\hat{\mathcal{R}} : \Omega^m \rightarrow \mathbb{R}$. Formally, for a regularization strength λ , we run mini-batch

particle gradient descent on

$$\mathcal{L}_S(Z) := \sum_{S \in \mathcal{S}} \text{SW}_2^2(\mu_S[Z], \hat{\mu}_S) + \lambda \hat{\mathcal{R}}(Z), \quad (7)$$

where SW_2^2 is the squared sliced Wasserstein distance.

Computing the gradient of the SW_2^2 distance For computing the gradient, we leverage the fact that the 1-dimensional 2-Wasserstein distance between $g_{\#}^{\theta} \mu_S[Z] = \frac{1}{m} \sum_i \delta(y_i)$ and $g_{\#}^{\theta} \hat{\mu}_S = \frac{1}{m} \sum_i \delta(y'_i)$ with $y_i, y'_i \in \mathbb{R}$ has a closed-form expression

$$W_2^2(g_{\#}^{\theta} \mu_S[Z], g_{\#}^{\theta} \hat{\mu}_S) = \frac{1}{m} \sum_i (y_{[i]} - y'_{[i]})^2, \quad (8)$$

where $y_{[i]}$ (resp. $y'_{[i]}$) denotes the i -th largest element. Equation (8) and its gradient can be computed efficiently by running a sorting algorithm, which is parallelizable on modern GPU architectures. We then approximate the SW_2^2 using N_{MC} Monte Carlo samples for θ . Consequently, we achieve a runtime complexity of $O(|\mathcal{S}| \cdot N_{\text{MC}} \cdot m \log m)$ for obtaining the gradient of the first term in Equation (7).

Finalization step Finally, after running particle gradient descent for T iterations, we obtain the dataset $D_{\text{DP}} \in \mathcal{X}^m$ by mapping every final particle in $Z^{(T)}$ to the closest point in $\text{Emb}(\mathcal{X}) \subset \Omega$.

3.4. Privacy guarantees

We outline the privacy guarantees for the dataset D_{DP} generated using PrivPGD. Leveraging the data post-processing property ([Dwork & Roth, 2014](#)), we establish the following lemma:

Lemma 3.2. *Assume that the noisy marginals $\{\hat{\nu}_S\}_{S \in \mathcal{S}}$ and the regularization loss $\hat{\mathcal{R}}$ are generated from two independent (ϵ_1, δ_1) - and (ϵ_2, δ_2) -DP mechanisms. Then, the output of Algorithm 3, D_{DP} , is $(\epsilon_1 + \epsilon_2, \delta_1 + \delta_2)$ -DP.*

Following standard practices in the literature ([McKenna et al., 2021; 2022; Vietri et al., 2022](#)), we employ the Gaussian mechanism to generate both the noisy marginals and the (parameterized) regularization loss for the experiments described in the next section. This approach ensures that the synthesized dataset D_{DP} adheres to differential privacy guarantees.

4. Experiments

In this section, we present a systematic large-scale experimental evaluation of our algorithm.

4.1. Experimental setting

Dataset We use 9 real-world datasets from various sources, detailed in Appendix A. Each dataset contains no

fewer than 50,000 data points, ranges from 3 to 22 dimensions and is linked to a binary classification or regression task, which we use to evaluate the downstream error. For these evaluations, we allocate 80% of the data as private data D and use the remaining 20% for test data D_{test} . We discretize every dimension containing real values or integer values exceeding a range of 32 into 32 equally-sized bins.

Privacy Budget We use $\epsilon = 2.5$ and $\delta = 10^{-5}$ as default choices. According to the National Institute of Standards and Technology (NIST), ϵ values below 5 can be considered as strong privacy protection and real-world applications commonly use values above 2.5 (Near & Darais, 2022).

Metrics We evaluate the statistical and downstream task performance of our algorithm with the following standard metrics for DP data synthesis:

1. *downstream error*: The classification/regression test error, i.e., the 0-1 (resp. mean squared) error, of gradient boosting trained on the synthesized data D_{DP} and evaluated on the (non-privatized) test dataset D_{test} .
2. *covariance error*: The Frobenius norm of the differences of the centered covariance matrices of $\text{Emb}(D)$ and $\text{Emb}(D_{DP})$ divided by the Frobenius norm of the centered covariance matrix of $\text{Emb}(D_{DP})$. Since the embedding just rescales the (discretized) variables, this is equivalent to computing the covariance matrix error of the normalized data, up to a constant.

Moreover, we use the relative average over $J = 200$ query differences between D_{DP} and D

$$\frac{\frac{1}{J} \sum_j |\text{query}_j(D_{DP}) - \text{query}_j(D)|}{\frac{1}{J} \sum_j \text{query}_j(D)}. \quad (9)$$

We instantiate the query difference for two commonly used queries (see e.g., (Vietri et al., 2022)):

3. *count. queries*: 3-sparse counting queries with $\text{query}_j(D) = \text{count}_j(D) = \frac{1}{n} \sum_i \mathbb{1}[x_i \in A_j]$ with A_j the full hypercube $\forall l : A_j^l = 1, \dots, k_l$ except for 3 random dimensions where the A_j^l is an interval with uniformly drawn lower bound and subsequently drawn upper bound. We use rejection sampling to ensure that at least 5% and at most 95% of the samples of the original dataset fall in this interval for every j .
4. *thresh. queries*: 3-sparse linear thresholding queries with $\text{query}_j(D) = \text{thrs}_j(D) = \frac{1}{n} \sum_i \mathbb{1}_{\langle x_i, \theta \rangle + b_j > 0}$; θ is a random 3-sparse direction and b_j is uniformly drawn from the interval $[\min_{x \in D} \langle x, \theta \rangle, \max_{x \in D} \langle x, \theta \rangle]$.

Finally, we compute the average sliced Wasserstein distance and the total variation distance. The former is approximately minimized by PrivPGD while the latter by existing marginal-based approaches (e.g., (McKenna et al., 2021; 2022)):

5. *average SW_1 dist.*: The average SW_1 distance over all 2-Way marginals between the embedded empirical probability measures of the original dataset D and the DP dataset D_{DP} ; $\mu_S[D], \mu_S[D_{DP}] \in \mathcal{P}(\text{Emb}(\mathcal{X})_S)$:

$$\binom{d}{2}^{-1} \sum_{S \subset [d]; |S|=2} SW_1(\mu_S[D], \mu_S[D_{DP}]). \quad (10)$$

6. *average TV dist.*: The average total variation distance TV over all 2-Way marginals between the original dataset D and the DP dataset D_{DP}

$$\binom{d}{2}^{-1} \sum_{S \subset [d]; |S|=2} TV(\nu_S[D], \nu_S[D_{DP}]). \quad (11)$$

Implementation of PrivPGD We implement PrivPGD using *PyTorch* and use the same hyperparameters for all experiments. We select all 2-Way marginals and use the Gaussian mechanism to construct DP-copies of them (step 2 in Algorithm 1). We then generate a dataset by running PrivPGD (Algorithm 3) with $100k$ particles.

For the *projection step* (Section 3.2), we use 200 MC random projections to approximate the SW_1 distance. We construct the finite measure $\hat{\omega}_{S, \mathbb{P}}$ by running gradient descent for 1750 iterations using Adam with an initial learning rate of 0.1 and a linear learning rate scheduler with step size 100 and multiplicative factor 0.8. As initialization, we use the probability measure obtained when setting all negative weights of $\hat{\omega}_S$ to zero and subsequently normalize the positive finite measure.

In the *optimization step* (Section 3.3), we approximate the SW_2^2 using $N_{MC} = 10$ projections. We minimize the objective in Equation (7) by running gradient descent for 1000 epochs (where in every epoch every marginal is seen exactly once) using an initial learning rate of 0.1 and a linear learning rate scheduler with step size 50 and multiplicative factor 0.75. We divide \mathcal{S} into mini-batches of size 5 and randomly set 80% of the gradient entries to zero. We use *Sparse Adam* from the *PyTorch* package.

Implementation of the metrics We use the implementation from *scikit-learn* (Buitinck et al., 2013) for Gradient Boosting using the standard hyperparameters. Since discretization is a separate problem on its own, we use the discretized dataset in all experiments.

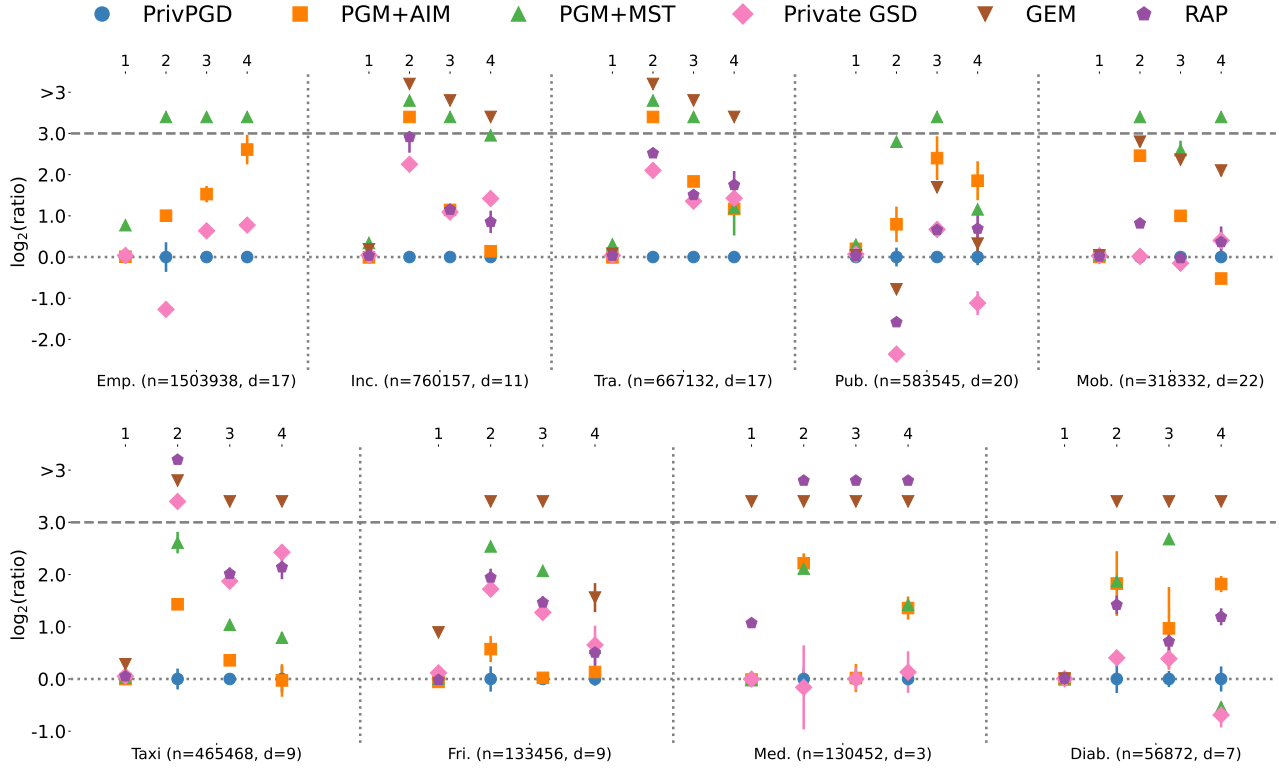


Figure 1. Comparison of PrivPGD with all 2-Way marginals against state-of-the-art methods based on metrics from Section 4.1: 1) downstream error, 2) covariance error, 3) count. queries error, and 4) thresh. queries error, across 9 tabular datasets. We plot the \log_2 ratio of the errors, using PrivPGD’s average error as the denominator, and report the mean and standard deviation over 5 runs. We cut at a log ratio of $y = 3$ (dashed line) and list all methods exceeding this threshold above this line in order. We set $\epsilon = 2.5$ and $\delta = 10^{-5}$.

4.2. Algorithms for benchmarking

We benchmark PrivPGD against a number of baselines including representative PGM-based and query-based methods. The PGM-based methods include MST (McKenna et al., 2021) and AIM (McKenna et al., 2022). For AIM, we choose all 2-Way marginals as workload. The following query-based algorithms include Private GSD (Liu et al., 2023), RAP (Aydore et al., 2021) and GEM (Liu et al., 2021), where we choose all 2-Way marginals as queries.

Implementation of AIM and MST. We implement MST and AIM using the code provided by the authors⁴. We choose the initial learning rate to be 1.0 and run mirror descent for 3000 iterations in every epoch. For AIM, we set the default maximum model size to 80Mb. We fix the hyperparameters for all experiments. Moreover, we slightly modify the code for MST and AIM by increasing the sensitivity used in the Gaussian (Dwork & Roth, 2014) and exponential mechanisms (McSherry & Talwar, 2007) to give accurate privacy guarantees for the differential privacy model from Definition 2.1. We refer to (McKenna et al., 2022) for an overview of both mechanisms in the context of DP data release.

⁴<https://github.com/ryan112358/private-pgm>.

Implementation of query-based algorithms. We use the one-shot version of Private GSD from the paper with an elite size of 2 and early stopping, and tune the number of generations $G \in \{200k, 500k\}$, the mutation and crossover populations $P_{mut} = P_{cross} \in \{50, 100, 150, 200, 500\}$, and the number of synthesized data points $m \in \{2k, 100k\}$. For GEM, we keep the default hyperparameters, tuning the number of iterations $T \in \{3, 10, 30, 50, 100, 150, 200\}$ and the model architecture $layers_{MLP} \in \{\{512, 512, 1024\}, \{128, 256\}\}$. For RAP, we also keep the default hyperparameters and tune $T \in \{3, 10, 30, 50, 100, 150, 200\}$, the learning rate $lr \in \{0.0001, 0.001, 0.03\}$ and $m \in \{2k, 500k\}$. This hyperparameter optimization includes the configurations considered by Liu et al. (2023). All methods are implemented using their official versions, with hyperparameters fine-tuned for each dataset. GEM and RAP could not be run for the ACS Employment dataset due to exceeding our memory constraint of 20 GB.

4.3. Comparison with baselines

We now present how the performance of PrivPGD compares against the state-of-the-art algorithms for DP data synthesis. Figure 1 illustrates the performance of PrivPGD compared

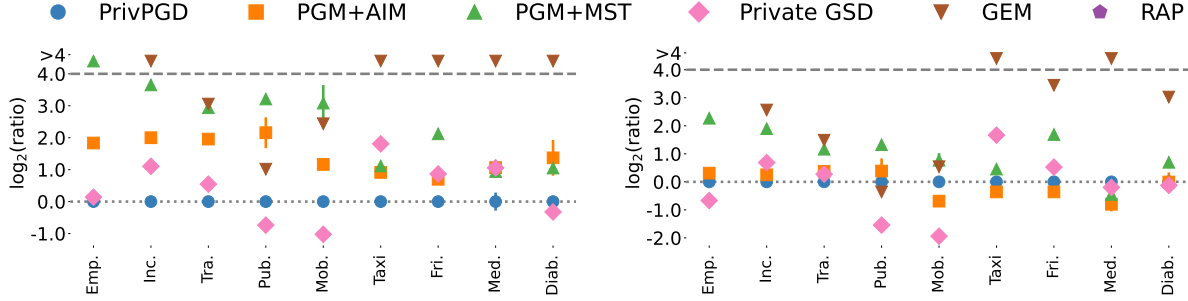


Figure 2. Comparison of average SW_1 distance (left) and average TV distance (right) for PrivPGD against state-of-the-art methods across 9 tabular datasets. We report the mean and standard deviation (5 runs) of the \log_2 ratio of errors. We set $\epsilon = 2.5$ and $\delta = 10^{-5}$.

to other methods, using metrics from Section 4.1. PrivPGD consistently ranks as either the best or the second-best in most metrics and datasets, with a few exceptions, such as the covariance error in the ACS Public Coverage dataset.

Comparison with PGM PrivPGD systematically outperforms both variants of PGM, which are the state-of-the-art for marginal-based tabular data synthesis, often by a significant margin. Specifically, it is better than PGM+MST in covariance and query errors across datasets, except for thresholding query errors in the Diabetes dataset, and performs at least as well as PGM+AIM, usually surpassing it, with the notable exception of thresholding query errors in the ACS Mobility dataset. For downstream tasks, PrivPGD performs comparably to PGM+AIM and consistently better than PGM+MST.

Comparison with query-based algorithms Furthermore, PrivPGD is also the preferred method in most scenarios when compared to query-based approaches, especially against GEM and RAP. While Private GSD provides competitive performance and occasionally surpasses PrivPGD – for instance, in the ACS Public Coverage dataset – PrivPGD usually emerges as the best-performing method. On many datasets it significantly outperforms Private GSD in all metrics, as exemplified by the Taxi, Black Friday, and ACS Traveltime datasets.

SW_1 and TV distance Finally, Figure 2 illustrates the performance gap between PrivPGD and other methods when comparing the average sliced Wasserstein distance and the total variation distance. PrivPGD effectively minimizes the former, while state-of-the-art methods like PGM primarily target the latter. Our experiments demonstrate the advantage of minimizing a geometry-aware loss function like the sliced Wasserstein distance over the total variation distance.

4.4. Enforcing additional domain-specific constraints

Section 4.3 shows that PrivPGD constructs a private dataset that successfully preserves the relevant statistics of the original dataset. However, while differential privacy protects individual information, many applications require the protection of specific population-level statistics, i.e., one would like specific statistics from the DP-dataset D_{DP} to have a large *mismatch* with statistics from the original dataset D . This goal is in contrast to the utility loss that tries to match certain statistics of the original dataset. One example is census data, where it might be desirable to hide religious or sexual orientations at the subpopulation level to prevent potential discriminatory misuse of the data. Another example is the publication of rental and house sale prices, where exposing certain correlations could lead to speculative abuses in specific locales.

We now demonstrate how PrivPGD, while constructing a high-quality dataset, also allows the protection of statistics on a population level. As an example, we consider maximizing the distance of a single linear (non-sparse) thresholding query $\text{thrs}_{\text{Emb}}(Z) = \frac{1}{m} \sum_i \mathbb{1}_{\langle Z_i, \theta \rangle + b > 0}$ defined directly in the embedding space. We approximate this query using a differentiable sigmoid approximation and define $\hat{\mathcal{R}}(Z) = \frac{1}{c + (\Delta(Z))^2}$ where $\Delta(Z)$ is the difference to a DP-estimate of the original data. We refer to the Appendix B for implementation details.

We plot in Figure 3 the absolute thresholding error as a function of the regularization strength λ . While the query is well approximated if no (or only little) regularization is used, we see how increasing the regularization strength increasingly protects these statistics, as the domain-specific counting query on D_{DP} deviates strongly from the one on the original data D . We further plot the downstream error and the absolute errors over random counting and thresholding queries (only the numerator in Equation (9)). We observe that, even for larger regularization penalties, these statistics are still preserved, comparable to the unregularized case.

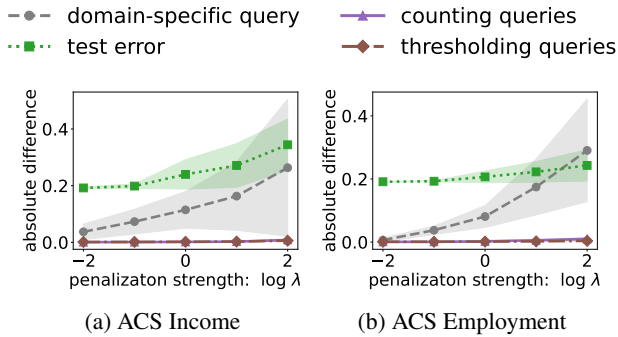


Figure 3. The absolute error of the domain-specific query (larger is better), the downstream classification error (smaller is better), and the absolute error over counting and thresholding queries (smaller is better), i.e., only the numerator in Equation 9, as a function of the log regularization strength λ . We plot the curves for (a) the Income and (b) the Employment dataset.

5. Conclusion and Future Work

We introduced PrivPGD, a novel generation method for marginal-based private data synthesis. Our approach leverages particle gradient descent, combined with techniques from optimal transport, resulting in improved performance in a large number of settings, enhanced scalability for handling numerous marginals and larger datasets, and increased flexibility for accommodating domain-specific constraints compared to existing methods.

Future work could develop regularization penalties that promote an inductive bias in PrivPGD towards more favorable solutions, similar to the maximum entropy bias in PGM. Additionally, exploring the design of domain-specific differentiable constraints and applying our method in practical scenarios presents an exciting avenue for future research.

Acknowledgements

KD was supported by the ETH AI Center and the ETH Foundations of Data Science. JA was supported by the ETH AI Center. We thank Aram Alexandre Pooladin and Guillaume Wang for insightful discussions.

Impact statement

This paper presents work whose goal is to advance the fields of Machine Learning and Privacy. There are many potential societal consequences of our work, none of which we feel must be specifically highlighted here.

References

Abowd, J. M. The US Census Bureau adopts differential privacy. In *Proceedings of the 24th ACM SIGKDD international conference on knowledge discovery & data*

mining, pp. 2867–2867, 2018.

Aktay, A., Bavadekar, S., Cossoul, G., Davis, J., Desfontaines, D., Fabrikant, A., Gabrilovich, E., Gadepalli, K., Gipson, B., Guevara, M., et al. Google COVID-19 community mobility reports: anonymization process description (version 1.1). *arXiv preprint arXiv:2004.04145*, 2020.

Asghar, H. J., Ding, M., Rakotoarivelo, T., Mrabet, S., and Kaafar, M. A. Differentially private release of high-dimensional datasets using the Gaussian copula. *arXiv preprint arXiv:1902.01499*, 2019.

Aydore, S., Brown, W., Kearns, M., Kenthapadi, K., Melis, L., Roth, A., and Siva, A. A. Differentially private query release through adaptive projection. In *Proceedings of the International Conference on Machine Learning*, pp. 457–467, 2021.

Boedihardjo, M., Strohmer, T., and Vershynin, R. Private measures, random walks, and synthetic data. *arXiv preprint arXiv:2204.09167*, 2022.

Bonneel, N., Rabin, J., Peyré, G., and Pfister, H. Sliced and Radon Wasserstein barycenters of measures. *Journal of Mathematical Imaging and Vision*, 51:22–45, 2015.

Buitinck, L., Louppe, G., Blondel, M., Pedregosa, F., Mueller, A., Grisel, O., Niculae, V., Prettenhofer, P., Gramfort, A., Grobler, J., Layton, R., VanderPlas, J., Joly, A., Holt, B., and Varoquaux, G. API design for machine learning software: experiences from the scikit-learn project. In *ECML PKDD Workshop: Languages for Data Mining and Machine Learning*, pp. 108–122, 2013.

Cai, K., Lei, X., Wei, J., and Xiao, X. Data synthesis via differentially private Markov random fields. *Proceedings of the VLDB Endowment*, 14(11):2190–2202, 2021.

Cao, T., Bie, A., Vahdat, A., Fidler, S., and Kreis, K. Don’t generate me: Training differentially private generative models with sinkhorn divergence. *Advances in Neural Information Processing Systems*, 34:12480–12492, 2021.

Chizat, L. Sparse optimization on measures with over-parameterized gradient descent. *Mathematical Programming*, 194(1):487–532, 2022.

Chizat, L. and Bach, F. On the global convergence of gradient descent for over-parameterized models using optimal transport. *Advances in neural information processing systems*, 31, 2018.

Dankar, F. K. and El Emam, K. The application of differential privacy to health data. In *Proceedings of the 2012 Joint EDBT/ICDT Workshops*, pp. 158–166, 2012.

- Deshpande, I., Zhang, Z., and Schwing, A. G. Generative modeling using the sliced Wasserstein distance. In *Proceedings of the IEEE conference on computer vision and pattern recognition*, pp. 3483–3491, 2018.
- Deshpande, I., Hu, Y.-T., Sun, R., Pyrros, A., Siddiqui, N., Koyejo, S., Zhao, Z., Forsyth, D., and Schwing, A. G. Max-sliced Wasserstein distance and its use for GANs. In *Proceedings of the IEEE/CVF Conference on Computer Vision and Pattern Recognition*, pp. 10648–10656, 2019.
- DiMaggio, C. *SAS for epidemiologists: applications and methods*. Springer, 2013.
- Ding, F., Hardt, M., Miller, J., and Schmidt, L. Retiring Adult: New datasets for fair machine learning. *Advances in Neural Information Processing Systems*, 34, 2021.
- Donhauser, K., Lokna, J., Sanyal, A., Boedihardjo, M., Höning, R., and Yang, F. Certified private data release for sparse Lipschitz functions, 2023.
- Dwork, C. Differential privacy. In *Automata, Languages and Programming*, pp. 1–12, 2006.
- Dwork, C. and Nissim, K. Privacy-preserving datamining on vertically partitioned databases. In *Advances in Cryptology—CRYPTO 2004: International Cryptology Conference*, pp. 528–544, 2004.
- Dwork, C. and Roth, A. The algorithmic foundations of differential privacy. *Foundations and Trends in Theoretical Computer Science*, 9(3–4):211–407, 2014.
- El Emam, K. The case for de-identifying personal health information. *SSRN Electronic Journal*, 2011.
- Gaboardi, M., Arias, E. J. G., Hsu, J., Roth, A., and Wu, Z. S. Dual Query: Practical private query release for high dimensional data. In *Proceedings of the International Conference on Machine Learning*, volume 32, pp. 1170–1178, 22–24 Jun 2014.
- Gambis, S., Ladouceur, F., Laurent, A., and Roy-Gaumond, A. Growing synthetic data through differentially-private vine copulas. *Proc. Priv. Enhancing Technol.*, 2021(3): 122–141, 2021.
- Grinsztajn, L., Oyallon, E., and Varoquaux, G. Why do tree-based models still outperform deep learning on typical tabular data? *Advances in Neural Information Processing Systems*, 35:507–520, 2022.
- Hardt, M., Ligett, K., and Mcsherry, F. A simple and practical algorithm for differentially private data release. In *Advances in Neural Information Processing Systems*, volume 25, 2012.
- Hu, Y., Wu, F., Li, Q., Long, Y., Garrido, G. M., Ge, C., Ding, B., Forsyth, D., Li, B., and Song, D. SoK: Privacy-preserving data synthesis. In *2024 IEEE Symposium on Security and Privacy (SP)*. IEEE Computer Society, may 2024. doi: 10.1109/SP54263.2024.00002.
- Johnson, N., Near, J. P., and Song, D. Towards practical differential privacy for SQL queries. *Proceedings of the VLDB Endowment*, 11(5):526–539, 2018.
- Jordon, J., Yoon, J., and Van Der Schaar, M. PATE-GAN: Generating synthetic data with differential privacy guarantees. In *Proceedings of the International conference on learning representations*, 2019.
- Kolouri, S., Rohde, G. K., and Hoffmann, H. Sliced Wasserstein distance for learning gaussian mixture models. In *Proceedings of the IEEE Conference on Computer Vision and Pattern Recognition*, pp. 3427–3436, 2018.
- Li, H., Xiong, L., and Jiang, X. Differentially private synthesis of multi-dimensional data using copula functions. In *Advances in database technology: proceedings. International conference on extending database technology*, volume 2014, pp. 475. NIH Public Access, 2014.
- Li, N., Zhang, Z., and Wang, T. DPSyn: Experiences in the NIST differential privacy data synthesis challenges. *Journal of Privacy and Confidentiality*, 11, 2021.
- Liu, T., Vietri, G., and Wu, S. Z. Iterative methods for private synthetic data: Unifying framework and new methods. *Advances in Neural Information Processing Systems*, 34:690–702, 2021.
- Liu, T., Tang, J., Vietri, G., and Wu, S. Generating private synthetic data with genetic algorithms. In *Proceedings of the 40th International Conference on Machine Learning*, volume 202 of *Proceedings of Machine Learning Research*, pp. 22009–22027, 23–29 Jul 2023.
- McKenna, R., Sheldon, D., and Miklau, G. Graphical-model based estimation and inference for differential privacy. In *International Conference on Machine Learning*, pp. 4435–4444. PMLR, 2019.
- McKenna, R., Miklau, G., and Sheldon, D. Winning the NIST contest: A scalable and general approach to differentially private synthetic data. *Journal of Privacy and Confidentiality*, 2021.
- McKenna, R., Mullins, B., Sheldon, D., and Miklau, G. AIM: An adaptive and iterative mechanism for differentially private synthetic data. *Proc. VLDB Endow.*, 15(11):2599–2612, jul 2022. ISSN 2150-8097. doi: 10.14778/3551793.3551817.

- McSherry, F. and Talwar, K. Mechanism design via differential privacy. In *IEEE Symposium on Foundations of Computer Science*, pp. 94–103, 2007.
- Near, J. and Darais, D. Differential privacy: Future work & open challenges, 2022. Accessed on 11th October 2023.
- Rakotomamonjy, A. and Liva, R. Differentially private sliced wasserstein distance. In *International Conference on Machine Learning*, pp. 8810–8820. PMLR, 2021.
- Sebag, I., PYDI, M. S., Franceschi, J.-Y., Rakotomamonjy, A., Gartrell, M., Atif, J., and Allauzen, A. Differentially private gradient flow based on the sliced wasserstein distance for non-parametric generative modeling. *arXiv preprint arXiv:2312.08227*, 2023.
- Strack, B., DeShazo, J. P., Gennings, C., Olmo, J. L., Ventura, S., Cios, K. J., Clore, J. N., et al. Impact of HbA1c measurement on hospital readmission rates: analysis of 70,000 clinical database patient records. *BioMed research international*, 2014, 2014.
- Tao, Y., McKenna, R., Hay, M., Machanavajjhala, A., and Miklau, G. Benchmarking differentially private synthetic data generation algorithms. *arXiv preprint arXiv:2112.09238*, 2021.
- Torkzadehmahani, R., Kairouz, P., and Paten, B. DP-CGAN: Differentially private synthetic data and label generation. In *Proceedings of the IEEE/CVF Conference on Computer Vision and Pattern Recognition Workshops*, 2019.
- Vallender, S. S. Calculation of the Wasserstein distance between probability distributions on the line. *Theory of Probability & Its Applications*, 18(4):784–786, 1974.
- Vero, M., Balunović, M., and Vechev, M. Programmable synthetic tabular data generation. *arXiv preprint arXiv:2307.03577*, 2023.
- Vietri, G., Tian, G., Bun, M., Steinke, T., and Wu, S. New oracle-efficient algorithms for private synthetic data release. In *Proceedings of the International Conference on Machine Learning*, pp. 9765–9774, 2020.
- Vietri, G., Archambeau, C., Aydore, S., Brown, W., Kearns, M., Roth, A., Siva, A., Tang, S., and Wu, S. Z. Private synthetic data for multitask learning and marginal queries. *Advances in Neural Information Processing Systems*, 35: 18282–18295, 2022.
- Wu, J., Huang, Z., Acharya, D., Li, W., Thoma, J., Paudel, D. P., and Gool, L. V. Sliced Wasserstein generative models. In *Proceedings of the IEEE/CVF Conference on Computer Vision and Pattern Recognition*, pp. 3713–3722, 2019.
- Xie, L., Lin, K., Wang, S., Wang, F., and Zhou, J. Differentially private generative adversarial network. *arXiv preprint arXiv:1802.06739*, 2018.
- Zhang, J., Xiao, X., and Xie, X. PrivTree: A differentially private algorithm for hierarchical decompositions. In *Proceedings of the international conference on management of data*, pp. 155–170, 2016.
- Zhang, J., Cormode, G., Procopiuc, C. M., Srivastava, D., and Xiao, X. PrivBayes: Private data release via Bayesian networks. *ACM Transactions on Database Systems (TODS)*, 42(4):1–41, 2017.
- Zhang, Z., Wang, T., Li, N., Honorio, J., Backes, M., He, S., Chen, J., and Zhang, Y. PrivSyn: Differentially private data synthesis. In *30th USENIX Security Symposium (USENIX Security 21)*, pp. 929–946, 2021.

A. Extended Experimental Details

Datasets We use a diverse range of real-world datasets, each with associated classification or regression tasks. Notably, our data sources include the American Community Survey (ACS) and various datasets from (Grinsztajn et al., 2022).

- **ACS Income classification dataset (Inc.) (Ding et al., 2021)**. The dataset focuses on predicting whether an individual earns more than 50,000 dollars annually. It is derived from the ACS PUMS data sample, with specific filters applied: only individuals aged above 16, those who reported working for at least 1 hour weekly in the past year, and those with a reported income exceeding 100 dollars were included. We take the data from California over a 5-year horizon and survey year 2018, with $d = 11$ dimension and $n = 760,157$ data points.
- **ACS Employment classification dataset (Emp.) (Ding et al., 2021)**. The dataset is designed to predict an individual’s employment status. It’s derived from the ACS PUMS data sample but only considers individuals aged between 16 and 90. We take the data from California over a 5-year horizon and survey year 2018, with $d = 17$ dimension and $n = 1,503,938$ data points.
- **ACS Mobility classification dataset (Mob.) (Ding et al., 2021)**. The goal is to determine if an individual retained the same residential address from the previous year using a filtered subset of the ACS PUMS data. This subset exclusively includes individuals aged between 18 and 35. Filtering for this age range heightens the prediction challenge, as over 90% of the broader population typically remains at the same address from one year to the next. We take the data from California over a 5-year horizon and survey year 2018, with $d = 22$ dimension and $n = 318,332$ data points.
- **ACS Traveltime classification dataset (Tra.) (Ding et al., 2021)**. The objective is to predict if an individual’s work commute surpasses 20 minutes using a refined subset of the ACS PUMS data. This subset is limited to those who are employed and are older than 16 years. The 20-minute benchmark was selected based on its status as the median travel time to work for the US population in the 2018 ACS PUMS data release. We take the data from California over a 5-year horizon and survey year 2018, with $d = 17$ dimension and $n = 667,132$ data points.
- **ACS Public Coverage classification dataset (Pub.) (Ding et al., 2021)**. The task is to predict if an individual is enrolled in public health insurance using a specific subset of the ACS PUMS data. This subset is narrowed down to individuals younger than 65 and with an income below 30,000 dollars. By focusing on this group, the prediction centers on low-income individuals who don’t qualify for Medicare. We take the data from California over a 5-year horizon and survey year 2018, with $d = 20$ dimension and $n = 583,545$ data points.
- **Medical charges regression dataset (Med.) (Grinsztajn et al., 2022)**. The dataset from the tabular benchmark, part of the “regression on numerical features” benchmark, details inpatient discharges under the Medicare fee-for-service scheme. Known as the Inpatient Utilization and Payment Public Use File (Inpatient PUF), it provides insights into utilization, total and Medicare-specific payments, and hospital-specific charges. The dataset encompasses data from over 3,000 U.S. hospitals under the Medicare Inpatient Prospective Payment System (IPPS) framework. Organized by hospitals and the Medicare Severity Diagnosis Related Group (MS-DRG), this dataset spans from Fiscal Year 2011 to 2016. In total, it contains $n = 130,452$ data point with $d = 3$ features.
- **Black Friday regression dataset (Fri.) (Grinsztajn et al., 2022)**. This dataset contains purchases from $n = 133,456$ buyers on black Friday. Each point is described by $d = 9$ features, including gender, age, occupation and marital status.
- **NYC Taxi Green December 2016 regression dataset (Taxi) (Grinsztajn et al., 2022)**. The dataset, utilized in the “regression on numerical features” benchmark from the tabular data benchmark, originates from the New York City Taxi and Limousine Commission’s (TLC) trip records for the green line in December 2016. In this processed version, string datetime details have been converted to numeric columns. The goal is to predict the “tip amount”. Records exclusively from credit card payments were retained. The dataset contains $n = 465,468$ points with $d = 9$ features.
- **Diabetes 130-US dataset classification dataset (Diab.) (Strack et al., 2014)**. The dataset encapsulates a decade (1999-2008) of $n = 56,872$ clinical observations from 130 US hospitals and integrated delivery systems, comprising over $d = 7$ features denoting patient and hospital results. The data was curated based on specific criteria: the record must be of an inpatient hospital admission, be associated with a diabetes diagnosis, have a stay duration ranging from 1 to 14 days, include laboratory tests, and involve medication administration.

B. Additional Details for Section 4.4

We now give additional descriptions for the experiments in Section 4.4. We approximate the thresholding function $\text{thr}_{\text{Emb}}(Z) = \frac{1}{m} \sum_i \mathbb{1}_{\langle Z_i, \theta \rangle + b > 0}$ using the smooth sigmoid approximation $\text{s-thr}_{\text{Emb}}(Z) = \frac{1}{m} \sum_i (1 + \exp(-s(\langle \theta, Z_i \rangle - b)))^{-1}$ with $s = 5.0$. We then split the privacy budget into two parts; the first part $\epsilon = 0.5$ and $\delta = 2 \times 10^{-6}$ is used for obtaining a DP estimate of $\text{s-thr}_{\text{Emb}}(\text{Emb}(D))$ using the Gaussian mechanism, which we denote by $\widehat{\text{s-thr}}_{\text{Emb}}$. Moreover, we use the remaining privacy budget $\epsilon = 2.0$ and $\delta = 8 \times 10^{-6}$ to privatize all 2-Way marginals using the Gaussian mechanism as in Algorithm 1. As a result, using the simple composition theorem (see e.g., (Dwork & Nissim, 2004)), the overall algorithm is then DP for $\epsilon = 2.5$ and $\delta = 10^{-5}$.

Finally, we generate the differentially private dataset D_{DP} by running Algorithm 3 with all privatized 2-Way marginals as inputs as well as the DP regularization loss

$$\hat{\mathcal{R}}(Z) = \frac{0.01}{0.0001 + (\text{s-thr}_{\text{Emb}}(Z) - \widehat{\text{s-thr}}_{\text{Emb}})^2}. \quad (12)$$

and regularization strength λ reaching from 10^{-2} to 10, as depicted in Figure 3.

C. Extended Results for Section 4.3

We replicate Figure 1 with $\epsilon = 1.0$ (see Figure 4) and $\epsilon = 0.2$ (see Figure 5). At smaller values of ϵ , PrivPGD is more frequently outperformed by PGM, especially in combination with AIM, and also with MST at $\epsilon = 0.2$, as well as more often by Private GSD. PGM-based methods benefit from a strong inductive bias towards maximum entropy solutions, which becomes particularly advantageous when noise levels are high. Nevertheless, PrivPGD still maintains highly competitive performance, especially in larger datasets and with fewer features. A similar trend is observed in the total variation and Wasserstein distance, as shown in Figures 6 and 7. These results underscore that PrivPGD’s performance edge diminishes as ϵ decreases.

Finally, Tables 1 to 6 provide the detailed metrics for all our results.

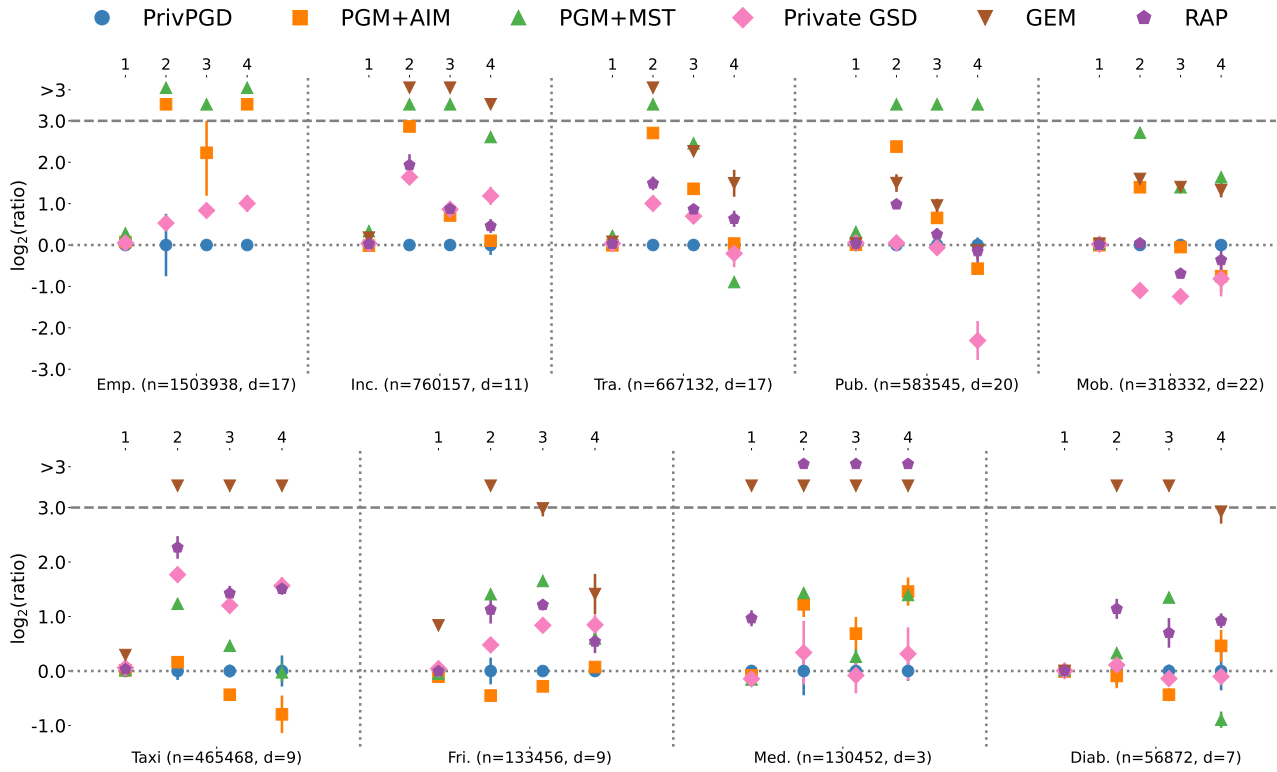


Figure 4. Comparison of PrivPGD with all 2-Way marginals against state-of-the-art methods based on metrics from Section 4.1: 1) downstream error, 2) covariance error, 3) count. queries error, and 4) thresh. queries error, across 9 tabular datasets. For each method, we plot the \log_2 ratio of the errors, using PrivPGD’s average error as the denominator, and report the mean and standard deviation over 5 runs. We cut at a log ratio of $y = 3$ (dashed line) and list all methods exceeding this threshold above this line in order. We set $\epsilon = 1.0$ and $\delta = 10^{-5}$.

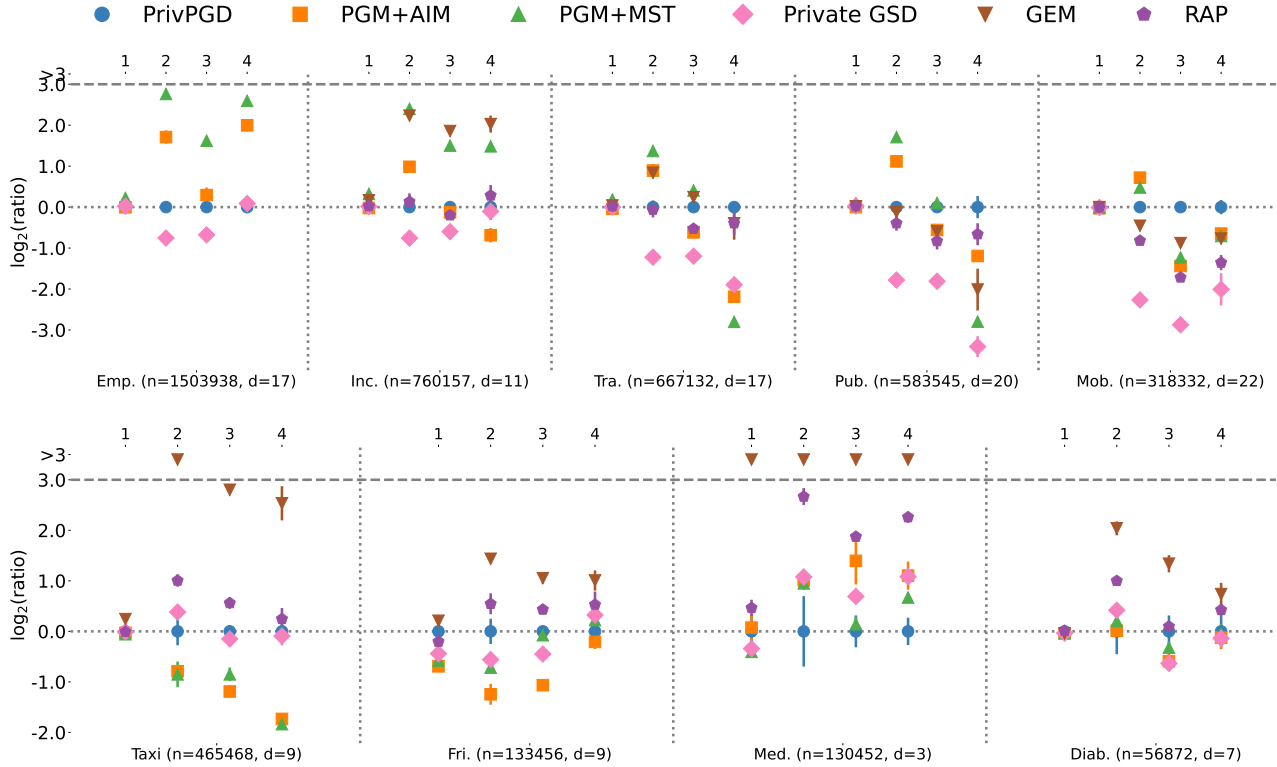


Figure 5. Comparison of PrivPGD with all 2-Way marginals against state-of-the-art methods based on metrics from Section 4.1: 1) downstream error, 2) covariance error, 3) count. queries error, and 4) thresh. queries error, across 9 tabular datasets. For each method, we plot the \log_2 ratio of the errors, using PrivPGD’s average error as the denominator, and report the mean and standard deviation over 5 runs. We cut at a log ratio of $y = 3$ (dashed line) and list all methods exceeding this threshold above this line in order. We set $\epsilon = 0.2$ and $\delta = 10^{-5}$.

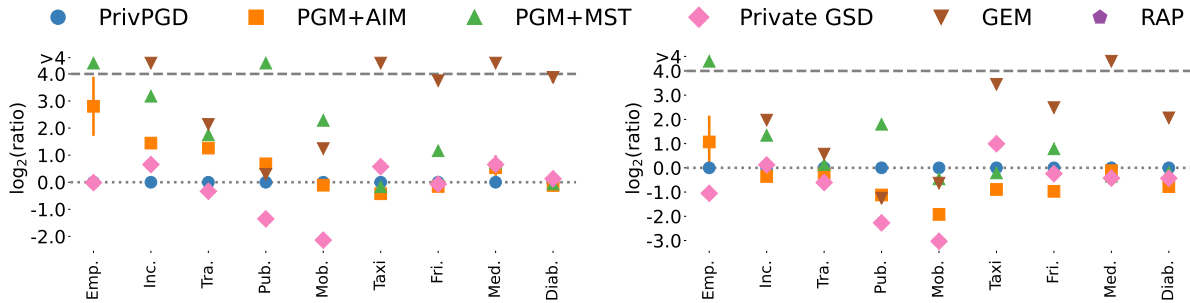


Figure 6. Comparison of average SW_1 distance (left) and average TV distance (right) for PrivPGD against state-of-the-art methods across 9 tabular datasets. Similar to Figure 1, we report the mean and standard deviation (5 runs) of the \log_2 ratio of errors. We set $\epsilon = 1.0$ and $\delta = 10^{-5}$.

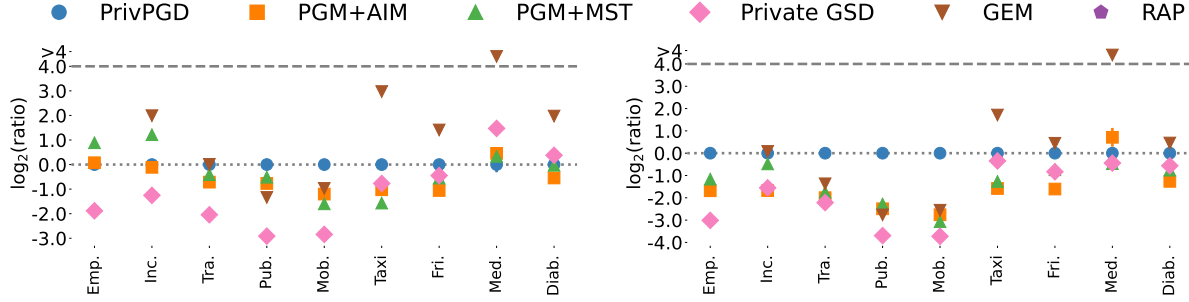


Figure 7. Comparison of average SW_1 distance (left) and average TV distance (right) for PrivPGD against state-of-the-art methods across 9 tabular datasets. Similar to Figure 1, we report the mean and standard deviation (5 runs) of the \log_2 ratio of errors. We set $\epsilon = 0.2$ and $\delta = 10^{-5}$.

dataset	inference	downstream	covariance	counting query	thresholding query	SW_1 distance	TV distance
Emp.	PrivPGD	0.19/0.19	0.02	0.00087	0.00043	0.00054	0.021
	PGM+AIM	0.19/0.19	0.04	0.0025	0.0026	0.0019	0.026
	PGM+MST	0.33/0.19	0.27	0.012	0.0075	0.0087	0.1
	Private GSD	0.2/0.19	0.0083	0.0013	0.00073	0.00059	0.013
Inc.	PrivPGD	0.19/0.19	0.001	0.00078	0.00031	0.00043	0.028
	PGM+AIM	0.19/0.19	0.014	0.0017	0.00034	0.0017	0.034
	PGM+MST	0.24/0.19	0.051	0.0077	0.0024	0.0054	0.11
	Private GSD	0.2/0.19	0.0049	0.0017	0.00083	0.00093	0.045
	GEM	0.22/0.19	0.047	0.01	0.0038	0.0099	0.17
	RAP	0.2/0.19	0.0078	0.0017	0.00056	0.0011	0.037
Tra.	PrivPGD	0.37/0.34	0.0026	0.00065	0.00014	0.00049	0.027
	PGM+AIM	0.37/0.34	0.037	0.0023	0.00031	0.0019	0.035
	PGM+MST	0.46/0.34	0.091	0.0058	0.00032	0.0038	0.061
	Private GSD	0.38/0.34	0.011	0.0017	0.00037	0.00072	0.033
	GEM	0.4/0.34	0.048	0.0052	0.0011	0.0041	0.076
	RAP	0.38/0.34	0.015	0.0019	0.00047	0.0014	0.036
Pub.	PrivPGD	0.28/0.27	0.06	0.00097	0.00033	0.00094	0.037
	PGM+AIM	0.32/0.27	0.1	0.0051	0.0012	0.0042	0.048
	PGM+MST	0.35/0.27	0.41	0.01	0.00074	0.0088	0.092
	Private GSD	0.3/0.27	0.012	0.0016	0.00015	0.00057	0.013
	GEM	0.29/0.27	0.035	0.0031	0.00042	0.0019	0.029
	RAP	0.29/0.27	0.02	0.0015	0.00054	0.0012	0.02
Mob.	PrivPGD	0.23/0.22	0.0091	0.0014	0.00051	0.0011	0.056
	PGM+AIM	0.23/0.22	0.05	0.0029	0.00036	0.0025	0.035
	PGM+MST	0.24/0.22	0.29	0.0088	0.005	0.0095	0.096
	Private GSD	0.24/0.22	0.0092	0.0013	0.00068	0.00055	0.015
	GEM	0.24/0.22	0.063	0.0074	0.0022	0.006	0.082
	RAP	0.23/0.22	0.016	0.0014	0.00066	0.0013	0.022

Table 1. The mean of the errors from Section 4 averaged over 5 runs. For the downstream error, we additionally show the test error when training on the original private dataset. We choose $\epsilon = 2.5$ and $\delta = 10^{-5}$.

dataset	inference	downstream	covariance	counting query	thresholding query	SW_1 distance	TV distance
Taxi	PrivPGD	2.3/2.2	0.00048	0.00051	0.00011	0.00027	0.02
	PGM+AIM	2.3/2.2	0.0013	0.00066	0.00011	0.0005	0.016
	PGM+MST	2.3/2.2	0.0029	0.0011	0.0002	0.00058	0.028
	Private GSD	2.3/2.2	0.004	0.0019	0.00061	0.00093	0.064
	GEM	2.7/2.2	0.079	0.016	0.0037	0.018	0.36
	RAP	2.3/2.2	0.0065	0.0021	0.0005	0.0013	0.078
Fri.	PrivPGD	1.5/1.4	0.00097	0.00064	0.00053	0.00033	0.015
	PGM+AIM	1.5/1.4	0.0014	0.00064	0.00058	0.00054	0.011
	PGM+MST	1.5/1.4	0.0057	0.0027	0.0008	0.0014	0.047
	Private GSD	1.7/1.4	0.0032	0.0015	0.00083	0.0006	0.021
	GEM	2.8/1.4	0.031	0.0066	0.0016	0.009	0.16
	RAP	1.5/1.4	0.0038	0.0018	0.00075	0.0011	0.034
Med.	PrivPGD	2.2/2.1	0.00014	0.0012	0.00013	0.00036	0.023
	PGM+AIM	2.1/2.1	0.00066	0.0012	0.00034	0.00076	0.013
	PGM+MST	2.1/2.1	0.00061	0.0012	0.00035	0.0007	0.017
	Private GSD	2.2/2.1	0.00013	0.0012	0.00014	0.00076	0.02
	GEM	75/2.1	0.11	0.1	0.054	0.22	1.4
	RAP	4.5/2.1	0.0048	0.013	0.0023	0.007	0.062
Diab.	PrivPGD	0.4/0.4	0.0013	0.0013	0.00042	0.00084	0.028
	PGM+AIM	0.4/0.4	0.0045	0.0025	0.0015	0.0022	0.028
	PGM+MST	0.41/0.4	0.0047	0.0083	0.00029	0.0017	0.045
	Private GSD	0.41/0.4	0.0017	0.0017	0.00026	0.00067	0.026
	GEM	0.41/0.4	0.042	0.032	0.0084	0.032	0.23
	RAP	0.41/0.4	0.0034	0.0021	0.00097	0.0025	0.041

Table 2. The mean of the errors from Section 4 averaged over 5 runs. For the downstream error, we additionally show the test error when training on the original private dataset. We choose $\epsilon = 2.5$ and $\delta = 10^{-5}$.

dataset	inference	downstream	covariance	counting query	thresholding query	SW ₁ distance	TV distance
Emp.	PrivPGD	0.19/0.19	0.0056	0.00077	0.00038	0.0006	0.027
	PGM+AIM	0.2/0.19	0.063	0.0036	0.004	0.0042	0.057
	PGM+MST	0.23/0.19	0.48	0.098	0.081	0.14	0.7
	Private GSD	0.2/0.19	0.008	0.0014	0.00076	0.00059	0.013
Inc.	PrivPGD	0.19/0.19	0.0019	0.00092	0.00039	0.0006	0.042
	PGM+AIM	0.19/0.19	0.014	0.0015	0.00042	0.0016	0.033
	PGM+MST	0.24/0.19	0.052	0.0077	0.0024	0.0054	0.11
	Private GSD	0.2/0.19	0.0061	0.0017	0.00089	0.00095	0.046
	GEM	0.22/0.19	0.047	0.01	0.0037	0.0098	0.16
	RAP	0.19/0.19	0.0074	0.0017	0.00054	0.001	0.041
Tra.	PrivPGD	0.37/0.34	0.0055	0.0011	0.00032	0.00091	0.05
	PGM+AIM	0.37/0.34	0.036	0.0027	0.00033	0.0022	0.042
	PGM+MST	0.44/0.34	0.073	0.0058	0.00017	0.0031	0.055
	Private GSD	0.38/0.34	0.011	0.0017	0.00028	0.00072	0.033
	GEM	0.4/0.34	0.048	0.0051	0.00091	0.004	0.074
	RAP	0.38/0.34	0.016	0.0019	0.0005	0.0016	0.041
Pub.	PrivPGD	0.28/0.27	0.011	0.0015	0.00061	0.0014	0.061
	PGM+AIM	0.28/0.27	0.058	0.0024	0.00041	0.0023	0.028
	PGM+MST	0.35/0.27	0.29	0.024	0.0092	0.04	0.21
	Private GSD	0.29/0.27	0.012	0.0014	0.00012	0.00055	0.013
	GEM	0.29/0.27	0.031	0.0029	0.00056	0.0017	0.025
	RAP	0.29/0.27	0.022	0.0018	0.00055	0.0014	0.023
Mob.	PrivPGD	0.23/0.22	0.021	0.0029	0.00085	0.0026	0.13
	PGM+AIM	0.23/0.22	0.054	0.0028	0.00051	0.0024	0.034
	PGM+MST	0.24/0.22	0.13	0.0077	0.0027	0.013	0.093
	Private GSD	0.24/0.22	0.0096	0.0012	0.00049	0.0006	0.016
	GEM	0.24/0.22	0.062	0.0077	0.0021	0.0062	0.083
	RAP	0.23/0.22	0.021	0.0018	0.00066	0.0017	0.031

Table 3. The mean of the errors from Figures 4 and 6 averaged over 5 runs. For the downstream error, we additionally show the test error when training on the original private dataset. We choose $\epsilon = 1.0$ and $\delta = 10^{-5}$.

dataset	inference	downstream	covariance	counting query	thresholding query	SW_1 distance	TV distance
Taxi	PrivPGD	2.3/2.2	0.0013	0.00077	0.00018	0.00062	0.033
	PGM+AIM	2.3/2.2	0.0014	0.00057	0.00011	0.00046	0.018
	PGM+MST	2.3/2.2	0.003	0.0011	0.00018	0.00055	0.029
	Private GSD	2.4/2.2	0.0043	0.0018	0.00055	0.00092	0.066
	GEM	2.8/2.2	0.081	0.017	0.0045	0.021	0.36
	RAP	2.3/2.2	0.0061	0.0021	0.00052	0.0014	0.08
Fri.	PrivPGD	1.6/1.4	0.0022	0.00086	0.00053	0.00068	0.028
	PGM+AIM	1.5/1.4	0.0016	0.00071	0.00056	0.00061	0.014
	PGM+MST	1.5/1.4	0.0058	0.0027	0.00081	0.0015	0.049
	Private GSD	1.6/1.4	0.0031	0.0015	0.00096	0.00065	0.024
	GEM	2.8/1.4	0.031	0.0068	0.0014	0.0092	0.16
	RAP	1.6/1.4	0.0048	0.002	0.00078	0.0016	0.046
Med.	PrivPGD	2.4/2.1	0.00032	0.0015	0.00019	0.00061	0.03
	PGM+AIM	2.3/2.1	0.00076	0.0024	0.00053	0.00088	0.027
	PGM+MST	2.1/2.1	0.00088	0.0018	0.00051	0.001	0.023
	Private GSD	2.2/2.1	0.00041	0.0014	0.00024	0.00095	0.022
	GEM	75/2.1	0.11	0.1	0.054	0.22	1.4
	RAP	4.7/2.1	0.0051	0.013	0.0024	0.007	0.066
Diab.	PrivPGD	0.4/0.4	0.0033	0.0026	0.001	0.002	0.052
	PGM+AIM	0.4/0.4	0.0031	0.0019	0.0014	0.0019	0.03
	PGM+MST	0.41/0.4	0.0042	0.0067	0.00056	0.0019	0.045
	Private GSD	0.41/0.4	0.0036	0.0024	0.00096	0.0022	0.039
	GEM	0.41/0.4	0.04	0.031	0.0078	0.03	0.22
	RAP	0.41/0.4	0.0073	0.0043	0.002	0.0054	0.071

Table 4. The mean of the errors from Figures 4 and 6 averaged over 5 runs. For the downstream error, we additionally show the test error when training on the original private dataset. We choose $\epsilon = 1.0$ and $\delta = 10^{-5}$.

dataset	inference	downstream	covariance	counting query	thresholding query	SW ₁ distance	TV distance
Emp.	PrivPGD	0.19 /0.19	0.015	0.0022	0.00078	0.0023	0.11
	PGM+AIM	0.19 /0.19	0.049	0.0027	0.0031	0.0024	0.035
	PGM+MST	0.23/0.19	0.1	0.0067	0.0047	0.0043	0.05
	Private GSD	0.2/0.19	0.0088	0.0014	0.00083	0.00063	0.014
Inc.	PrivPGD	0.19 /0.19	0.0098	0.0027	0.00086	0.0024	0.15
	PGM+AIM	0.19 /0.19	0.019	0.0025	0.00053	0.0022	0.048
	PGM+MST	0.24/0.19	0.052	0.0077	0.0024	0.0056	0.11
	Private GSD	0.2/0.19	0.0058	0.0018	0.0008	0.001	0.052
	GEM	0.22/0.19	0.046	0.0099	0.0035	0.0096	0.16
	RAP	0.2/0.19	0.011	0.0024	0.001	0.0019	0.072
Tra.	PrivPGD	0.38/0.34	0.027	0.0043	0.0012	0.004	0.19
	PGM+AIM	0.37 /0.34	0.05	0.0028	0.00027	0.0024	0.048
	PGM+MST	0.44/0.34	0.07	0.0058	0.00018	0.003	0.057
	Private GSD	0.38/0.34	0.012	0.0019	0.00033	0.00097	0.041
	GEM	0.4/0.34	0.048	0.0051	0.00093	0.004	0.073
	RAP	0.39/0.34	0.026	0.003	0.00093	0.0033	0.074
Pub.	PrivPGD	0.29 /0.27	0.048	0.0058	0.0021	0.0064	0.24
	PGM+AIM	0.29 /0.27	0.1	0.0039	0.00093	0.0037	0.043
	PGM+MST	0.31/0.27	0.16	0.0062	0.00031	0.0045	0.05
	Private GSD	0.29 /0.27	0.014	0.0017	0.0002	0.00085	0.019
	GEM	0.29 /0.27	0.044	0.0039	0.00053	0.0025	0.035
	RAP	0.29 /0.27	0.037	0.0033	0.0013	0.003	0.049
Mob.	PrivPGD	0.24/0.22	0.085	0.014	0.003	0.011	0.46
	PGM+AIM	0.23 /0.22	0.14	0.0052	0.0019	0.0049	0.068
	PGM+MST	0.24/0.22	0.12	0.006	0.0019	0.0037	0.054
	Private GSD	0.24/0.22	0.018	0.0019	0.00076	0.0016	0.035
	GEM	0.24/0.22	0.062	0.0076	0.0018	0.0058	0.078
	RAP	0.24/0.22	0.048	0.0043	0.0012	0.0048	0.08

Table 5. The mean of the errors from Figures 5 and 7 averaged over 5 runs. For the downstream error, we additionally show the test error when training on the original private dataset. We choose $\epsilon = 0.2$ and $\delta = 10^{-5}$.

dataset	inference	downstream	covariance	counting query	thresholding query	SW_1 distance	TV distance
Taxi	PrivPGD	2.4/2.2	0.0055	0.0025	0.00072	0.0026	0.11
	PGM+AIM	2.3 /2.2	0.0032	0.0011	0.00022	0.0013	0.037
	PGM+MST	2.3 /2.2	0.003	0.0014	0.0002	0.00087	0.046
	Private GSD	2.4/2.2	0.0071	0.0022	0.00068	0.0015	0.087
	GEM	2.8/2.2	0.082	0.017	0.0042	0.02	0.36
	RAP	2.4/2.2	0.011	0.0036	0.00086	0.0036	0.17
Fri.	PrivPGD	2.5/1.4	0.011	0.0031	0.00071	0.0031	0.11
	PGM+AIM	1.5 /1.4	0.0048	0.0015	0.00061	0.0015	0.036
	PGM+MST	1.6/1.4	0.0069	0.003	0.00082	0.0021	0.065
	Private GSD	1.8/1.4	0.0077	0.0023	0.00088	0.0023	0.061
	GEM	2.8/1.4	0.031	0.0065	0.0014	0.0083	0.15
	RAP	2.1/1.4	0.017	0.0042	0.001	0.0055	0.12
Med.	PrivPGD	3/2.1	0.0013	0.0048	0.00082	0.0024	0.076
	PGM+AIM	3.1/2.1	0.0027	0.013	0.0018	0.0033	0.12
	PGM+MST	2.2 /2.1	0.0026	0.0053	0.0013	0.0031	0.055
	Private GSD	2.3/2.1	0.0028	0.0078	0.0017	0.0067	0.056
	GEM	76/2.1	0.11	0.1	0.054	0.21	1.4
	RAP	4.1/2.1	0.0084	0.018	0.0039	0.01	0.1
Diab.	PrivPGD	0.42/0.4	0.01	0.013	0.0045	0.0082	0.17
	PGM+AIM	0.41 /0.4	0.011	0.0085	0.0042	0.0056	0.071
	PGM+MST	0.41 /0.4	0.012	0.01	0.0044	0.008	0.1
	Private GSD	0.41 /0.4	0.014	0.0083	0.0041	0.011	0.12
	GEM	0.41 /0.4	0.043	0.033	0.0076	0.032	0.23
	RAP	0.42/0.4	0.021	0.014	0.0061	0.018	0.19

Table 6. The mean of the errors from Figures 5 and 7 averaged over 5 runs. For the downstream error, we additionally show the test error when training on the original private dataset. We choose $\epsilon = 0.2$ and $\delta = 10^{-5}$.